scientific reports

Check for updates

OPEN

New equivalent resistance formula of $m \times n$ rectangular resistor network represented by Chebyshev polynomials

Ru Wang[1], Xiaoyu Jiang[1]✉, Yanpeng Zheng[2]✉, Zhaolin Jiang[3] & Deliang Xiang[2]

In the process of exploring the field of circuits, obtaining the exact solution of the equivalent resistance between two nodes in a resistor network has become an important problem. This paper aims to introduce Chebyshev polynomial of the second kind to improve the equivalent resistance formula of $m \times n$ rectangular resistor network, thereby improving the calculation efficiency. Additionally, the discrete sine transform of the first kind (*DST-I*) is utilized to solve the modeling equation. Under the condition of applying the new equivalent resistance formula, several equivalent resistance formulas with different parameters are given, and three-dimensional views are used to illustrate them. Six comparison tables are provided to showcase the advantages of the improved explicit formula in terms of computational efficiency, as well as the relationship between resistivity and the maximum size of the resistor network that the formula can effectively handle. This may provide more convenient and effective technical support for research and practice in electronic engineering and other related fields.

The resistor network is an important research direction in the field of circuit analysis and design. These play a vital role in various electronic systems and applications, and are widely used in signal processing, power systems, communication systems and so on. Accurate analysis and efficient calculation of the equivalent resistance in a resistor network is essential for understanding its behavior and optimizing performance. Tan's[1–10] innovative work in establishing various resistor network models has provided significant theoretical support and has far-reaching implications for scientific researchers. By improving the efficiency of calculating the equivalent resistance formula, researchers can better solve complex scientific and technical problems. Therefore, in order to enhance the numerical processing of the formula, this paper re-expresses the original formula using Chebyshev polynomials to save calculation time.

According to research, many practical problems have been solved by establishing resistor network models[11–18] and neural network models[20–27]. In the past few decades, researchers have extensively studied resistor networks, focusing on research directions such as electromigration phenomenon, graph theory, studies of impedance network, infinite network, finite network and the other Laplace matrix (*LM*) methods[17–19,28–41,43–46]. The neural network proposed by Shi et al.[20–23] has similarities with the resistor network in processing and analyzing complex systems.

In recent years, the Recursion-Transform (*RT*) method proposed by Tan[1–10,47–52] has attracted extensive attention in the research of resistor networks as a novel computational method. The *RT* method calculates the equivalent resistance by establishing a tridiagonal matrix and using matrix transformation and operation. Currently, there are many research results on tridiagonal matrices[53–63]. The traditional Green′s function method[41–43] is usually employed to solve infinite resistor network problems or those with periodic boundary conditions by calculating equivalent resistance through the construction of a point source in the network. The Green′s function approach relies on network symmetry and Fourier transforms, making it suited for obtaining analytical solutions in infinite or periodic networks. However, for finite networks, the resistance formulas derived from the Green's function method are less suitable for numerical computation, as the integral convergence slows with increasing grid points, thereby complicating the calculations. In contrast, the *RT* method is applicable to finite network models of various sizes and complexities, offering greater flexibility in engineering applications. In 2015, the method is further improved, Tan[2] studies the hard problem of two-point resistance on irregular $m \times n$ spider webs with an arbitrary longitude. Additionally, Tan conducted research and analysis on spherical[3] and

[1]School of Information Science and Engineering, Linyi University, Linyi 276000, China. [2]School of Automation and Electrical Engineering, Linyi University, Linyi 276000, China. [3]School of Mathematics and Statistics, Linyi University, Linyi 276000, China. ✉email: jxy19890422@sina.com; zhengyanpeng0702@sina.com

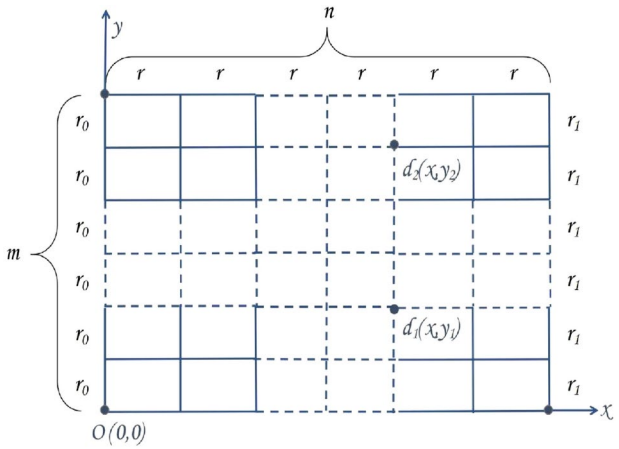

Fig. 1. An $m \times n$ rectangular resistor network, except the right boundary resistor in the vertical direction is r_1, its horizontal and vertical resistors are r and r_0, respectively.

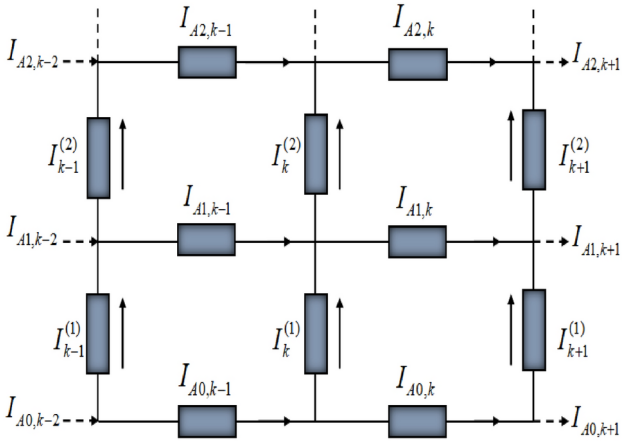

Fig. 2. Partial resistor network with current directions and parameters.

sector[8] network models. The *RT* method has become an important technical mean to study various topological resistor networks[1–10,47–52], which has the potential to bring new breakthroughs and development opportunities to the field of electronic engineering and other fields.

This paper is organized as follows: In Sect. 2, the original equivalent resistance formula of rectangular resistor network is given. In Sect. 3, a new formula of equivalent resistance expressed by Chebyshev polynomials is given. In Sect. 4, the derivation of the new formula is introduced in detail. In Sect. 5, the equivalent resistance formulas and their three-dimensional diagrams for several special cases are presented. In Sect. 6, the efficiency of the original formula and the new formula for calculating equivalent resistance is analyzed. In Sect. 7, the paper is concluded.

Original equivalent resistance formula

In this section, the equivalent resistance formula for an $m \times n$ resistor network with an arbitrary boundary, derived by Tan[7], is provided, along with the key equations necessary for solving it.

In 2016, Tan[7] proposed an $m \times n$ rectangular resistor network, as shown in Fig. 1. The resistance in the vertical and horizontal directions are r_0 and r, where r_1 is the right boundary resistor, m and n are the number of resistors between two nodes on each vertical line and horizontal line, respectively. r_1 is an arbitrary resistor on the right boundary. Various geometric structures can be obtained by adjusting the right boundary. For example, when $r_1 = 0$, a fan-shaped network model is obtained, and when $r_1 = r_0$, a regular rectangular network model is formed. The nodes in the resistor network are represented by coordinates (x, y). Where $d_1(x, y_1)$ and $d_2(x, y_2)$ are two arbitrary nodes on the common vertical axis of the $m \times n$ resistor network. A part of the rectangular resistor network is selected for analysis and study using Kirchhoff's law. The schematic diagram of the partial resistor network is shown in Fig. 2, which represents all current distributions and parameters in the resistor network.

The equivalent resistance $R_{m\times n}(d_1,d_2)$ between two arbitrary nodes $d_1(x,y_1)$ and $d_2(x,y_2)$ in an $m\times n$ rectangular resistor network is shown below

$$R_{m\times n}(d_1,d_2)=\frac{r_0}{m+1}\sum_{i=1}^{m}\frac{(C_{1,i}-C_{2,i})^2}{1-\cos\theta_i}\times\left(\frac{\left[\Delta F_{n-x}^{(i)}+(h_1-1)\Delta F_{n-x-1}^{(i)}\right]\Delta F_x^{(i)}}{F_{n+1}^{(i)}+(h_1-1)F_n^{(i)}}\right), \tag{1}$$

where

$$\begin{aligned} h_1=r_1/r_0,\ C_{k,i}=\cos(y_k+\frac{1}{2})\theta_i,\ \theta_i=\frac{i\pi}{m+1},\\ F_k^{(i)}=\left(\lambda_i^k-\bar{\lambda}_i^k\right)/(\lambda_i-\bar{\lambda}_i),\ \Delta F_k^{(i)}=F_{k+1}^{(i)}-F_k^{(i)}, \end{aligned} \tag{2}$$

$$\begin{aligned} \lambda_i&=1+h-h\cos\theta_i+\sqrt{(1+h-h\cos\theta_i)^2-1},\\ \bar{\lambda}_i&=1+h-h\cos\theta_i-\sqrt{(1+h-h\cos\theta_i)^2-1},\quad h=r/r_0. \end{aligned} \tag{3}$$

Tan analyzed and studied the resistor network, and established a resistor network model based on Kirchhoff's law. The general matrix equation is given below.

$$\mathrm{I}_{k+1}=\mathrm{A}_m\mathrm{I}_k-\mathrm{I}_{k-1}-J\mathrm{H}_x\delta_{k,x}, \tag{4}$$

the function $\delta_{k,x}$ is defined as $\delta_{k,x}=\begin{cases}1, & x=k\\ 0, & x\neq k\end{cases}$, I_k and H_x are the $m\times 1$ column matrices which can be described as

$$\begin{aligned} \mathrm{I}_k&=\left[I_k^{(1)},\ I_k^{(2)},\ ...,I_k^{(m)}\right]^T\ (0\le k\le n),\\ (\mathrm{H}_x)_j&=h(-\delta_{j,y_1}+\delta_{j,y_1+1}+\delta_{j,y_2}-\delta_{j,y_2+1}), \end{aligned}$$

where $(\mathrm{H}_x)_j$ is the element of H_x when injecting current J at $d_1(x,y_1)$ and exiting at $d_2(x,y_2)$,

$$\mathrm{A}_m=\begin{pmatrix} 2+2h & -h & 0 & \cdots & 0\\ -h & 2+2h & -h & \ddots & \vdots\\ 0 & \ddots & \ddots & \ddots & 0\\ \vdots & \ddots & -h & 2+2h & -h\\ 0 & \cdots & 0 & -h & 2+2h \end{pmatrix}_{m\times m}, \tag{5}$$

where $h=r/r_0$.

New formula of equivalent resistance represented by Chebyshev polynomials

For the equivalent resistance formula (1), Eq. (2) is an explanation of the symbols in formula (1), which involves complex exponential operations and has high computational complexity. In order to improve the calculation efficiency of equivalent resistance, this section introduces the improved equivalent resistance formula using the Chebyshev polynomial of the second kind.

Let the current J be input at $d_1(x,y_1)$ and output at $d_2(x,y_2)$, the equivalent resistance between two nodes in the $m\times n$ resistor network is given by

$$R_{m\times n}(d_1,d_2)=\frac{r_0}{m+1}\sum_{j=1}^{m}\frac{(S_{1,j}-S_{2,j})^2}{1-\cos\theta_j}\times\left(\frac{[\Delta B_{n-x}^{(j)}+(h_1-1)\Delta B_{n-x-1}^{(j)}]\Delta B_x^{(j)}}{B_{n+1}^{(j)}+(h_1-1)B_n^{(j)}}\right), \tag{6}$$

where

$$\Delta B_k^{(j)}=B_{k+1}^{(j)}-B_k^{(j)}, \tag{7}$$

$$\begin{aligned} S_{q,j}=\cos\frac{(q+\frac{1}{2})j\pi}{m+1},\ q=y_1,\ y_2,\\ \theta_j=\frac{j\pi}{m+1}, \end{aligned} \tag{8}$$

$$\begin{aligned} B_k^{(j)}=B_k^{(j)}(\cosh\mu_j)=\frac{\sinh(k\mu_j)}{\sinh\mu_j},\ \cosh\mu_j=\frac{\sigma_j}{2},\\ k=n-x+1,\ n-x,\ n-x-1,\ x+1,\ x,\ n+1,\ n,\quad j=1,\ 2,\ \ldots,\ m. \end{aligned} \tag{9}$$

$$\sigma_j = 2 + \frac{2r}{r_0} - \frac{2r}{r_0}\cos\frac{j\pi}{m+1}. \tag{10}$$

Derivation of the new equivalent resistance formula

In this section, Chebyshev polynomial of the second kind is adopted to signify the Horadam sequence[64], which improves the calculation efficiency. And the discrete sine transform is introduced to obtain the solution of the model equations, the equivalent resistance formula is re-derived.

Horadam sequence represented by Chebyshev polynomials

Horadam sequence contains the following conditions:

$$W_k = dW_{k-1} - qW_{k-2}, \quad W_0 = A, \quad W_1 = B, \tag{11}$$

where $k \in \mathrm{N}, \quad k \geq 2, \ A, \ B, \ d, \ q \in \mathrm{C}$, N is the set of all natural numbers and C is the set of all complex numbers.

Horadam sequence[65] represented by Chebyshev polynomial of the second kind is

$$W_k = (\sqrt{q})^k \left(\frac{B}{\sqrt{q}} U_{k-1}\left(\frac{d}{2\sqrt{q}}\right) - AU_{k-2}\left(\frac{d}{2\sqrt{q}}\right)\right), \tag{12}$$

where

$$U_k = \frac{\sin(k+1)\eta}{\sin\eta}, \quad \cos\eta = \frac{d}{2\sqrt{q}}, \quad \eta \in \mathrm{C}, \tag{13}$$

is the Chebyshev polynomial of the second kind[66].

Equation (13) contains complex numbers, since $\frac{d}{2\sqrt{q}} > 1$, which in this study can be described as

$$B_k = U_k = \frac{\sinh(k+1)\mu}{\sinh\mu}, \quad \cosh\mu = \frac{d}{2\sqrt{q}}, \quad \mu \in \mathrm{R}, \tag{14}$$

where $i\mu = \eta$, i is the imaginary unit.

Discrete sine transform

Let

$$\mathbb{S}_m^I = \sqrt{\frac{2}{m+1}}\left(\sin\frac{jk\pi}{m+1}\right)_{k,j=1}^{m}. \tag{15}$$

The matrix $\mathbb{S}_m^I$ is a well-known discrete sine transform of the first kind (*DST-I*)[67,68]. $\mathbb{S}_m^I$ is an orthogonal matrix, and the inverse and transpose of $\mathbb{S}_m^I$ are still itself, i.e.

$$(\mathbb{S}_m^I)^{-1} = (\mathbb{S}_m^I)^T = \mathbb{S}_m^I. \tag{16}$$

For Eq. (5), perform the following orthogonal diagonalization

$$(\mathbb{S}_m^I)^{-1}\mathrm{A}_m\mathbb{S}_m^I = \mathrm{diag}(\sigma_1, \ \sigma_2, \ \ldots, \ \sigma_m), \tag{17}$$

therefore,

$$\mathrm{A}_m = \mathbb{S}_m^I \mathrm{diag}(\sigma_1, \ \sigma_2, \ \ldots, \ \sigma_m)(\mathbb{S}_m^I)^{-1}, \tag{18}$$

where

$$\sigma_j = 2 + 2h - 2h\cos\frac{(j-1)\pi}{m}, \quad j = 1, \ 2, \ \ldots, \ m. \tag{19}$$

From Eq. (17), it is known that the matrix A_m is similar to $\mathrm{diag}(\sigma_1, \ \sigma_2, \ \ldots, \ \sigma_m)$, so σ_j is the eigenvalue of A_m.

By left-multiplying Eq. (17) by $\mathbb{S}_m^I$, we obtain the following equation

$$\mathrm{A}_m\mathbb{S}_m^I = \mathbb{S}_m^I \mathrm{diag}(\sigma_1, \ \sigma_2, \ \ldots, \ \sigma_m),$$

i.e.,

$$\mathrm{A}_m\left(\mathcal{T}^{(1)},\ \mathcal{T}^{(2)},\ \ldots,\ \mathcal{T}^{(m)}\right)=\left(\mathcal{T}^{(1)},\ \mathcal{T}^{(2)},\ \ldots,\ \mathcal{T}^{(m)}\right)\mathrm{diag}(\sigma_1,\ \sigma_2,\ \ldots,\ \sigma_m), \tag{20}$$

where $\mathcal{T}^{(j)}=\left(\mathcal{T}_1^{(j)},\ \mathcal{T}_2^{(j)},\ \ldots,\ \mathcal{T}_m^{(j)}\right)$,

$$\mathcal{T}_k^{(j)}=\sqrt{\frac{2}{m+1}}\sin\frac{jk\pi}{m+1},\quad k=1,\ 2,\ \ldots,\ m,\ j=1,\ 2,\ \ldots,\ m.$$

Equation (20) can be expressed as

$$\mathrm{A}_m\mathcal{T}^{(j)}=\sigma_j\mathcal{T}^{(j)},\quad j=1,\ 2,\ \ldots,\ m. \tag{21}$$

Based on Eq. (21), the eigenvector $\mathcal{T}^{(j)}=\left(\mathcal{T}_1^{(j)},\ \mathcal{T}_2^{(j)},\ \ldots,\ \mathcal{T}_m^{(j)}\right)$ corresponding to σ_j is obtained.

Let

$$\sqrt{\frac{m+1}{2}}\mathbb{S}_m^I\mathrm{I}_k=\mathrm{L}_k, \tag{22}$$

where the $m\times 1$ column matrix L_k is

$$\mathrm{L}_k=\left[L_k^{(1)},L_k^{(2)},...,L_k^{(m)}\right]^T\ (0\le k\le n).$$

According to Eqs. (16) and (22), it can be obtained as follows

$$\mathrm{I}_k=\sqrt{\frac{2}{m+1}}\mathbb{S}_m^I\mathrm{L}_k. \tag{23}$$

Considering the boundary conditions of the rectangular resistor network, the following current equations are established based on Kirchhoff's law

$$\mathrm{I}_1=[\mathrm{A}_m-\mathrm{E}_m]\mathrm{I}_0, \tag{24}$$

$$\begin{aligned}\mathrm{I}_{n-1}&=[\mathrm{A}_m-(2-h_1)\mathrm{E}_m]\mathrm{I}_n,\\ h_1\mathrm{I}_n+\mathrm{I}_{n-2}&=\mathrm{A}_m\mathrm{I}_{n-1},\end{aligned} \tag{25}$$

where $h_1=\frac{r_1}{r_0}$, A_m is given by Eq.(5) and E_m is the $m\times m$ identity matrix.

Equations (4), (24) and (25) are multiplied by $\sqrt{\frac{2}{m+1}}\mathbb{S}_m^I$ on the left, and then combine with Eq. (22) to obtain the following equations

$$L_{k+1}^{(j)}=\sigma_jL_k^{(j)}-L_{k-1}^{(j)}-Jh\delta_{k,x}\zeta_j, \tag{26}$$

$$\begin{aligned}L_1^{(j)}&=(\sigma_j-1)L_0^{(j)},\\ L_{n-1}^{(j)}&=(\sigma_j+h_1-2)L_n^{(j)},\end{aligned} \tag{27}$$

$$h_1L_n^{(j)}+L_{n-2}^{(j)}=\sigma_jL_{n-1}^{(j)}, \tag{28}$$

where

$$\zeta_j=2\sin(\frac{1}{2}\theta_j)\left[\left[\cos(y_1+\frac{1}{2})\theta_j-\cos(y_2+\frac{1}{2})\theta_j\right]\right]. \tag{29}$$

Solving the matrix equations

The homogeneous equation of Eq. (26) is expressed as follows

$$L_{k+1}^{(j)}=\sigma_jL_k^{(j)}-L_{k-1}^{(j)},$$

let $W_0=L_x$, $W_1=L_{x+1}$, $d=\sigma_j$ and $q=1$ in Eq. (11), combine Eqs. (12), (13) and (14) to get the following equation

$$L_k^{(j)}=L_{x+1}^{(j)}B_{k-x}^{(j)}-L_x^{(j)}B_{k-x-1}^{(j)}, \tag{30}$$

where

$$B_k^{(j)} = B_k^{(j)}(\cosh\mu_j) = \frac{\sinh(k\mu_j)}{\sinh\mu_j},\ \cosh\mu_j = \frac{\sigma_j}{2}, \tag{31}$$

σ_j is defined by Eq. (19).

Next, consider the solution of Eq. (26) with the current input at $d_1(x_1, y_1)$ and output at $d_2(x_2, y_2)$. According to Eq. (30), the piecewise solutions of Eq. (26) are obtained as follows

$$L_k^{(j)} = L_1^{(j)} B_k^{(j)} - L_0^{(j)} B_{k-1}^{(j)},\quad 0 \le k \le x, \tag{32}$$

$$L_{x+1}^{(j)} = \sigma_j L_x^{(j)} - L_{x-1}^{(j)} - Jh\zeta_j, \tag{33}$$

$$L_k^{(j)} = L_{x+1}^{(j)} B_{k-x}^{(j)} - L_x^{(j)} B_{k-x-1}^{(j)},\quad x \le k \le n, \tag{34}$$

where $B_k^{(j)}$ is defined by Eq. (31).

Based on Eqs. (27), (28), (32), (33) and (34), the expression of $L_x^{(j)}$ can be described as

$$L_x^{(j)} = Jh\frac{[(\sigma_j - 2)B_{n-x}^{(j)} + h_1\Delta B_{n-x-1}^{(j)}]\Delta B_x^{(j)}}{(\sigma_j - 2)(\Delta B_n^{(j)} + h_1 B_n^{(j)})}\zeta_j. \tag{35}$$

From Eqs. (15), (23) and (35), the sum of currents between two nodes can be expressed as

$$\sum_{j=y_1+1}^{y_2} I_x^{(j)} = \frac{J}{m+1}\sum_{j=1}^{m}\frac{(S_{1,j} - S_{2,j})^2}{1-\cos\theta_j} \times \left(\frac{[(\sigma_j - 2)B_{n-x}^{(j)} + h_1\Delta B_{n-x-1}^{(j)}]\Delta B_x^{(j)}}{\Delta B_n^{(j)} + h_1 B_n^{(j)}}\right). \tag{36}$$

According to Ohm's law, the equivalent resistance formula between two nodes is described as

$$R_{m\times n}(d_1, d_2) = \frac{1}{J}|U_{d_1} - U_{d_2}| = \frac{1}{J}\left(\sum_{j=y_1+1}^{y_2} I_x^{(j)}\right) r_0, \tag{37}$$

due to Eqs. (36) and (37), the explicit formula (6) for the equivalent resistance between two nodes can be obtained.

Demonstrating the equivalent resistance formulas for some special cases

Formula (6) is a general conclusion for rectangular resistor networks that includes all cases. The influence of different variables on the explicit equivalent resistance formula is analyzed from two aspects as follows, and 3D views are used to demonstrate them.

Influence of current input node on equivalent resistance

This part gives examples of the change of equivalent resistance when the current input node is different.

Case 1. Assume that the current J is input at node $d_1(x_1, y_1)(x_1 = x, y_1 = 0)$, and the current flows out of the resistor network at node $d_2(x_2, y_2)(x_2 = x, y_2 = y)$, the equivalent resistance between nodes d_1 and d_2 can be written as

$$R_{m\times n}(\{x,0\},\{x,y\}) = \frac{r_0}{m+1}\sum_{j=1}^{m}\frac{[\cos\frac{\theta_j}{2} - \cos(y+\frac{1}{2})\theta_j]^2}{1-\cos\theta_j} \times \left(\frac{[\Delta B_{n-x}^{(j)} + (h_1-1)\Delta B_{n-x-1}^{(j)}]\Delta B_x^{(j)}}{B_{n+1}^{(j)} + (h_1-1)B_n^{(j)}}\right),$$

where $\Delta B_k^{(j)}$, θ_j and $B_k^{(j)}$ are defined by Eqs. (7), (8) and (8), respectively.

When $m = n = 80,\ J = 10,\ y_1 = 0,\ r_0 = r = 1$ and $r_1 = 11$, in other words, $h_1 = 11$, the following formula is obtained

$$R_{80\times 80}(\{x,0\},\{x,y\}) = \frac{1}{81}\sum_{j=1}^{80}\frac{\left[\cos\frac{\theta_j}{2} - \cos(y+\frac{1}{2})\theta_j\right]^2}{1-\cos\theta_j} \times \left(\frac{(\Delta B_{80-x}^{(j)} + 10\Delta B_{79-x}^{(j)})\Delta B_x^{(j)}}{B_{81}^{(j)} + 10B_{80}^{(j)}}\right), \tag{38}$$

where

$$\Delta B_{80-x}^{(j)} = B_{81-x}^{(j)} - B_{80-x}^{(j)}, \tag{39}$$

$$\Delta B_{79-x}^{(j)} = B_{8-x}^{(j)} - B_{79-x}^{(j)}, \tag{40}$$

$$\theta_j = \frac{j\pi}{m+1}, \tag{41}$$

$$B_k^{(j)} = B_k^{(j)}(\cosh\mu_j) = \frac{\sinh(k\mu_j)}{\sinh\mu_j},\ \cosh\mu_j = 1 + \frac{r}{r_0} - \frac{r}{r_0}\cos\frac{j\pi}{m+1}, \tag{42}$$
$$k = 81 - x,\ 80 - x,\ 79 - x,\ x + 1,\ x,\ 81,\ 80,\quad j = 1,\ 2,\ \ldots,\ 80.$$

A three-dimensional view of Eq. (38) is shown in Fig. 3.

Case 2. If the current J is input at node $d_1(x_1, y_1)(x_1 = x, y_1 = 30)$ in the resistor network and output at node $d_2(x_2, y_2)(x_2 = x, y_2 = y)$, the equivalent resistance formula between d_1 and d_2 can be characterized as

$$R_{m\times n}(\{x,30\},\{x,y\}) = \frac{r_0}{m+1}\sum_{j=1}^{m}\frac{\left[\cos\frac{61\theta_j}{2} - \cos(y+\frac{1}{2})\theta_j\right]^2}{1-\cos\theta_j} \times \left(\frac{[\Delta B_{n-x}^{(j)} + (h_1-1)\Delta B_{n-x-1}^{(j)}]\Delta B_x^{(j)}}{B_{n+1}^{(j)} + (h_1-1)B_n^{(j)}}\right), \tag{43}$$

where $\Delta B_k^{(j)}$, θ_j and $B_k^{(j)}$ are defined by Eqs. (7), (8) and (8), respectively.

In a resistor network of size 80×80, when $J = 10,\ y_1 = 30,\ h_1 = 11$ and $r_0 = r = 1$, Eq. (43) is defined as

$$R_{80\times 80}(\{x,30\},\{x,y\}) = \frac{1}{81}\sum_{j=1}^{80}\frac{[\cos\frac{61\theta_j}{2} - \cos(y+\frac{1}{2})\theta_j]^2}{1-\cos\theta_j} \times \left(\frac{(\Delta B_{80-x}^{(j)} + 10\Delta B_{79-x}^{(j)})\Delta B_x^{(j)}}{B_{81}^{(j)} + 10B_{80}^{(j)}}\right), \tag{44}$$

where $\Delta B_{80-x}^{(j)}, \Delta B_{79-x}^{(j)}, \theta_j$ and $B_k^{(j)}$ $(k = 81 - x,\ 80 - x,\ 79 - x,\ x + 1,\ x,\ 81,\ 80,\quad j = 1,\ 2,\ \ldots,\ 80$) are the same as Eqs. (39), (40), (41) and (42), respectively.

A three-dimensional view of Eq. (44) is shown in Fig. 4.

Case 3. Assume that the current J is input into the resistor network, $d_1(x_1, y_1)(x_1 = x, y_1 = 80)$ is the input node of the current and $d_2(x_2, y_2)(x_2 = x, y_2 = y)$ is the output node, then the equivalent resistance formula between these two nodes can be expressed as

$$R_{m\times n}(\{x,80\},\{x,y\}) = \frac{r_0}{m+1}\sum_{j=1}^{m}\frac{[\cos\frac{161\theta_j}{2} - \cos(y+\frac{1}{2})\theta_j]^2}{1-\cos\theta_j} \times \left(\frac{[\Delta B_{n-x}^{(j)} + (h_1-1)\Delta B_{n-x-1}^{(j)}]\Delta B_x^{(j)}}{B_{n+1}^{(j)} + (h_1-1)B_n^{(j)}}\right), \tag{45}$$

where $\Delta B_k^{(j)}$, θ_j and $B_k^{(j)}$ are defined by Eqs. (7), (8) and (8), respectively.

When $J = 10,\ y_1 = 80,\ r_1 = 11$ and $r_0 = r = 1$, Eq. (45) is described in the resistor network of size 80×80 as

$$R_{80\times 80}(\{x,80\},\{x,y\}) = \frac{1}{81}\sum_{j=1}^{80}\frac{[\cos\frac{161\theta_j}{2} - \cos(y+\frac{1}{2})\theta_j]^2}{1-\cos\theta_j} \times \left(\frac{(\Delta B_{80-x}^{(j)} + 10\Delta B_{79-x}^{(j)})\Delta B_x^{(j)}}{B_{81}^{(j)} + 10B_{80}^{(j)}}\right), \tag{46}$$

where $\Delta B_{80-x}^{(j)}, \Delta B_{79-x}^{(j)}, \theta_j$ and $B_k^{(j)}$ $(k = 81 - x,\ 80 - x,\ 79 - x,\ x + 1,\ x,\ 81,\ 80,\quad j = 1,\ 2,\ \ldots,\ 80$) are the same as Eqs. (39), (40), (41) and (42), respectively.

A three-dimensional view of Eq. (46) is shown in Fig. 5.

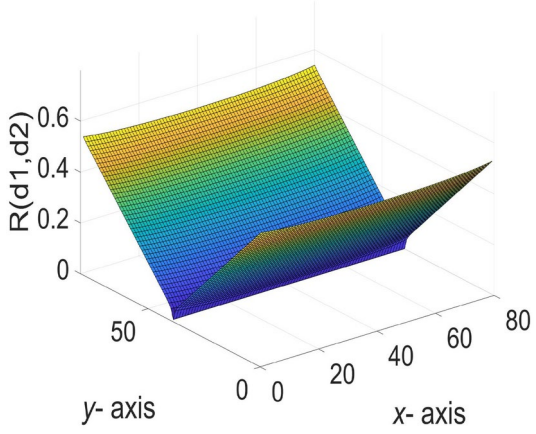

Fig. 3. The 3D equivalent resistance distribution diagram of $R_{80\times 80}(\{x,0\},\{x,y\})$ in Eq. (38).

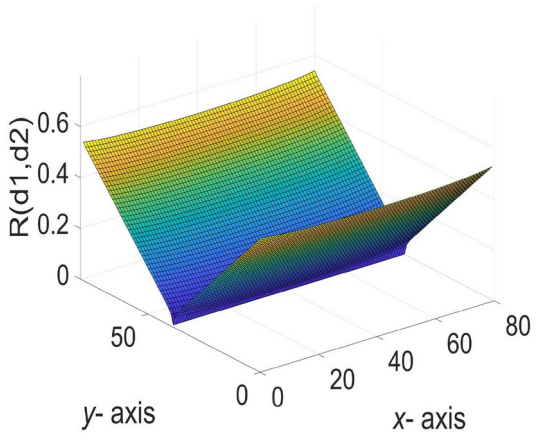

Fig. 4. The 3D equivalent resistance distribution diagram of $R_{80\times 80}(\{x,30\},\{x,y\})$ in Eq. (44).

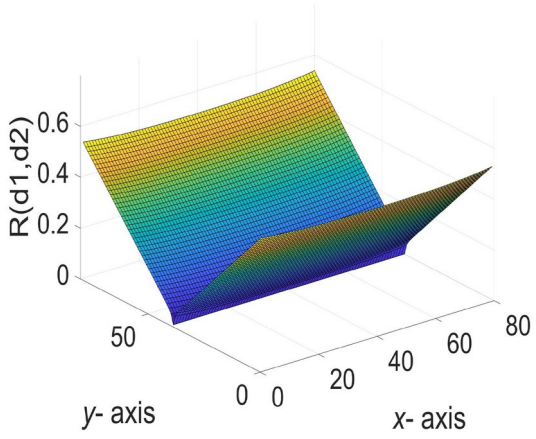

Fig. 5. The 3D equivalent resistance distribution diagram of $R_{80\times 80}(\{x,80\},\{x,y\})$ in Eq. (46).

Effect of resistivity h ($h=\frac{r}{r_0}$) on equivalent resistance

The following discusses the values of the equivalent resistance between nodes d_1 and d_2 on each vertical axis of the resistor network when the value of y_1 at the current input node d_1 remains constant and the resistivity h is different. The resistivity here is the ratio of r to r_0, denoted by h, i.e., $h=\frac{r}{r_0}$.

Case 4. If the node $d_1(x_1,y_1)(x_1=x,y_1=40)$ in the resistor network is used as the input node of the current J, and $d_2(x_2,y_2)(x_2=x,y_2=y)$ is used as the output node, then the equivalent resistance formula between the two nodes d_1 and d_2 is written as

$$R_{m\times n}(\{x,40\},\{x,y\})=\frac{r_0}{m+1}\sum_{j=1}^{m}\frac{[\cos\frac{81\theta_j}{2}-\cos(y+\frac{1}{2})\theta_j]^2}{1-\cos\theta_j}\times\left(\frac{[\Delta B^{(j)}_{n-x}+(h_1-1)\Delta B^{(j)}_{n-x-1}]\Delta B^{(j)}_{x}}{B^{(j)}_{n+1}+(h_1-1)B^{(j)}_{n}}\right),$$

where $\Delta B^{(j)}_k$, θ_j and $B^{(j)}_k$ are defined by Eqs. (7), (8) and (8), respectively.

When $m=n=80,\ J=10,\ y_1=40,\ r_1=11,\ r_0=1$ and $r=0.1$, the following formula is obtained

$$R_{80\times 80}(\{x,40\},\{x,y\})=\frac{1}{81}\sum_{j=1}^{80}\frac{[\cos\frac{161\theta_j}{2}-\cos(y+\frac{1}{2})\theta_j]^2}{1-\cos\theta_j}\times\left(\frac{(\Delta B^{(j)}_{80-x}+10\Delta B^{(j)}_{79-x})\Delta B^{(j)}_{x}}{B^{(j)}_{81}+10B^{(j)}_{80}}\right),\quad(47)$$

where $\Delta B^{(j)}_{80-x}$, $\Delta B^{(j)}_{79-x}$, θ_j and $B^{(j)}_k$ ($k=81-x,\ 80-x,\ 79-x,\ x+1,\ x,\ 81,\ 80,\ \ j=1,\ 2,\ \ldots,\ 80$) are the same as Eqs. (39), (40), (41) and (42), respectively.

A three-dimensional view of Eq. (47) is shown in Fig. 6.

Case 5. Assume that the current $J=10$ flows from a fixed input node $d_1(x_1,y_1)(x_1=x,y_1=40)$ to a fixed output node $d_2(x_2,y_2)(x_2=x,y_2=y)$ in a rectangular resistor network.

In this case, given $h_1=11,\ h=0.01$, in other words, $r_1=11,\ r_0=1,\ r=0.01$ the equivalent resistance formula between these two nodes is described as

$$R_{m\times n}(\{x,40\},\{x,y\}) = \frac{r_0}{m+1}\sum_{j=1}^{m}\frac{[\cos\frac{81\theta_j}{2}-\cos(y+\frac{1}{2})\theta_j]^2}{1-\cos\theta_j}\times\left(\frac{[\Delta B_{n-x}^{(j)}+(h_1-1)\Delta B_{n-x-1}^{(j)}]\Delta B_x^{(j)}}{B_{n+1}^{(j)}+(h_1-1)B_n^{(j)}}\right), \quad (48)$$

where $\Delta B_k^{(j)}$, θ_j and $B_k^{(j)}$ are defined by Eqs. (7), (8) and (8), respectively.

When the size of the resistor network is 80×80, ie $m=80,\ n=80$, Eq. (48) is represented as

$$R_{80\times 80}(\{x,40\},\{x,y\}) = \frac{1}{81}\sum_{j=1}^{80}\frac{[\cos\frac{161\theta_j}{2}-\cos(y+\frac{1}{2})\theta_j]^2}{1-\cos\theta_j}\times\left(\frac{(\Delta B_{80-x}^{(j)}+10\Delta B_{79-x}^{(j)})\Delta B_x^{(j)}}{B_{81}^{(j)}+10B_{80}^{(j)}}\right), \quad (49)$$

where $\Delta B_{80-x}^{(j)}, \Delta B_{79-x}^{(j)}, \theta_j$ and $B_k^{(j)}$ $(k=81-x,\ 80-x,\ 79-x,\ x+1,\ x,\ 81,\ 80,\quad j=1,\ 2,\ \ldots,\ 80$) are the same as Eqs. (39), (40), (41) and (42), respectively.

A three-dimensional view of Eq. (49) is shown in Fig. 7.

Case 6. Suppose the current $J=10$ flows into resistor network through $d_1(x_1,y_1)(x_1=x,y_1=40)$ and out at $d_2(x_2,y_2)(x_2=x,y_2=y)$, at this time, the equivalent resistance formula between d_1 and d_2 can be expressed as

$$R_{m\times n}(\{x,40\},\{x,y\}) = \frac{r_0}{m+1}\sum_{j=1}^{m}\frac{[\cos\frac{81\theta_j}{2}-\cos(y+\frac{1}{2})\theta_j]^2}{1-\cos\theta_j}\times\left(\frac{[\Delta B_{n-x}^{(j)}+(h_1-1)\Delta B_{n-x-1}^{(j)}]\Delta B_x^{(j)}}{B_{n+1}^{(j)}+(h_1-1)B_n^{(j)}}\right),$$

where $\Delta B_k^{(j)}$, θ_j and $B_k^{(j)}$ are defined by Eqs. (7), (8) and (8), respectively.

Let $m=n=80,\ h_1=11,\ h=0.001,$ that is , $r_1=11,\ r_0=1,\ r=0.001$ the following formula is obtained

$$R_{80\times 80}(\{x,40\},\{x,y\}) = \frac{1}{81}\sum_{j=1}^{80}\frac{[\cos\frac{161\theta_j}{2}-\cos(y+\frac{1}{2})\theta_j]^2}{1-\cos\theta_j}\times\left(\frac{(\Delta B_{80-x}^{(j)}+10\Delta B_{79-x}^{(j)})\Delta B_x^{(j)}}{B_{81}^{(j)}+10B_{80}^{(j)}}\right), \quad (50)$$

where $\Delta B_{80-x}^{(j)}, \Delta B_{79-x}^{(j)}, \theta_j$ and $B_k^{(j)}$ $(k=81-x,\ 80-x,\ 79-x,\ x+1,\ x,\ 81,\ 80,\quad j=1,\ 2,\ \ldots,\ 80$) are the same as Eqs. (39), (40), (41) and (42), respectively.

A three-dimensional view of Eq. (50) is shown in Fig. 8.

Calculation efficiency of different equivalent resistance formulas

In this section, examples are shown that demonstrate the computational efficiency of two equivalent resistor formulas. In the $m\times n$ rectangular resistor network, $d_1(x,y_1)$ and $d_2(x,y_2)$ represent the current input and output nodes, respectively. In the experiment, the y_1 value of the input node is fixed, and each y_2 node on each vertical axis is traversed. The CPU processing times t_1 and t_2 represent the time required to calculate the equivalent resistance using formula (1) and formula (6), respectively, and demonstrate the calculation efficiency of the two different formulas.

These experiments are done on an Intel Core i7-12700H laptop with 2.30 GHz CPU and NVIDIA GeForce RTX 3060 GPU. In the following tables, the calculation time is in seconds, "$m\times n$" denotes the scale of resistor network, "*" and the dashed empty bar indicate computer memory overflow.

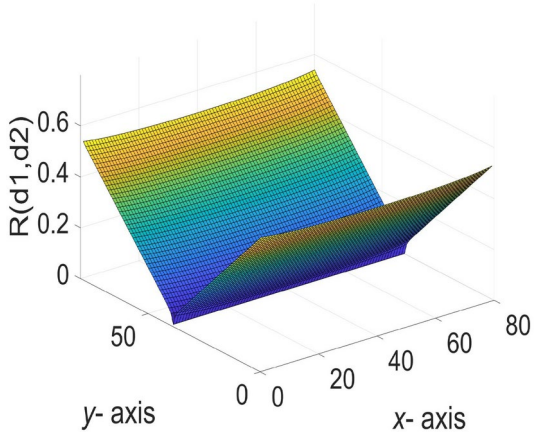

Fig. 6. The 3D equivalent resistance distribution diagram of $R_{80\times 80}(\{x,40\},\{x,y\})$ in Eq. (47).

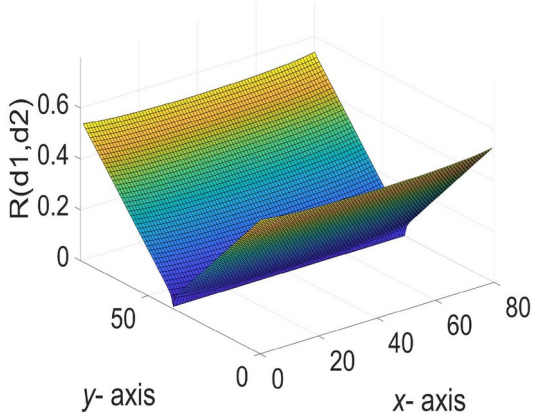

Fig. 7. The 3D equivalent resistance distribution diagram of $R_{80\times 80}(\{x,40\},\{x,y\})$ in Eq. (49).

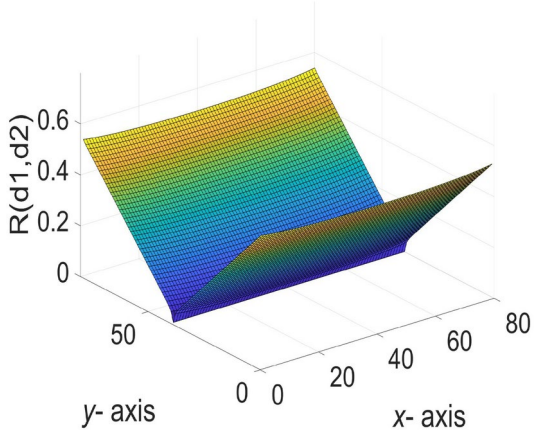

Fig. 8. The 3D equivalent resistance distribution diagram of $R_{80\times 80}(\{x,40\},\{x,y\})$ in Eq. (50).

When $y_1 = 30$, $r/r_0 = 1$, the CPU time spent calculating the equivalent resistance by formula (1) and formula (6), respectively is shown in Fig. 9.

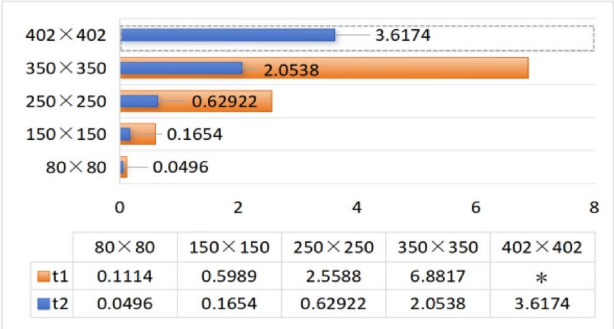

	80×80	150×150	250×250	350×350	402×402
t1	0.1114	0.5989	2.5588	6.8817	*
t2	0.0496	0.1654	0.62922	2.0538	3.6174

Fig. 9. CPU time to calculate equivalent resistance using formula (1) and formula (6), respectively.

When $y_1 = 30$, $r/r_0 = 0.1$, the CPU time spent calculating the equivalent resistance by formula (1) and formula (6), respectively is shown in Fig. 10.

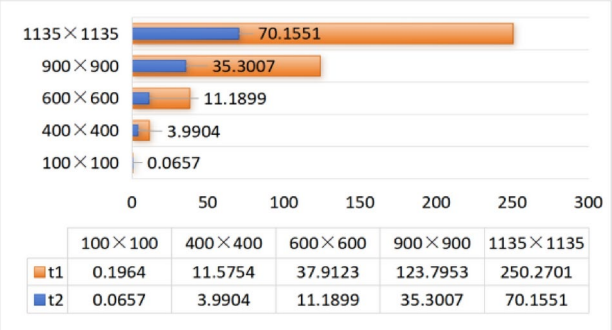

	100×100	400×400	600×600	900×900	1135×1135
t1	0.1964	11.5754	37.9123	123.7953	250.2701
t2	0.0657	3.9904	11.1899	35.3007	70.1551

Fig. 10. CPU time to calculate equivalent resistance using formula (1) and formula (6), respectively.

When $y_1 = 30$, $r/r_0 = 0.01$, the CPU time spent calculating the equivalent resistance by formula (1) and formula (6), respectively is shown in Fig. 11.

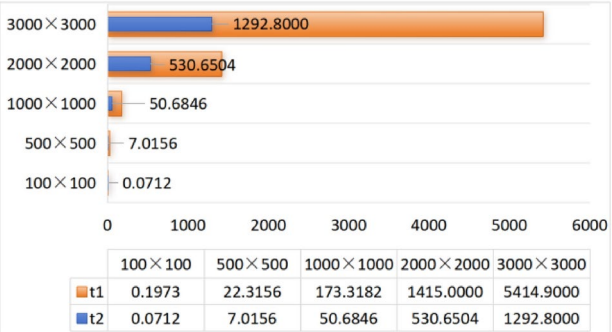

	100×100	500×500	1000×1000	2000×2000	3000×3000
t1	0.1973	22.3156	173.3182	1415.0000	5414.9000
t2	0.0712	7.0156	50.6846	530.6504	1292.8000

Fig. 11. CPU time to calculate equivalent resistance using formula (1) and formula (6), respectively.

When $y_1 = 50$, $r/r_0 = 1$, the CPU time spent calculating the equivalent resistance by formula (1) and formula (6), respectively is shown in Fig. 12.

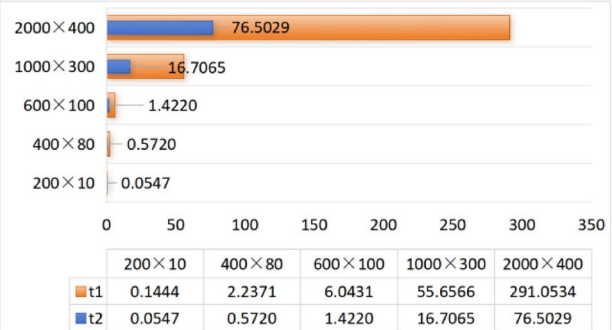

	200×10	400×80	600×100	1000×300	2000×400
t1	0.1444	2.2371	6.0431	55.6566	291.0534
t2	0.0547	0.5720	1.4220	16.7065	76.5029

Fig. 12. CPU time to calculate equivalent resistance using formula (1) and formula (6), respectively.

When $y_1 = 50$, $r/r_0 = 0.1$, the CPU time spent calculating the equivalent resistance by formula (1) and formula (6), respectively is shown in Fig. 13.

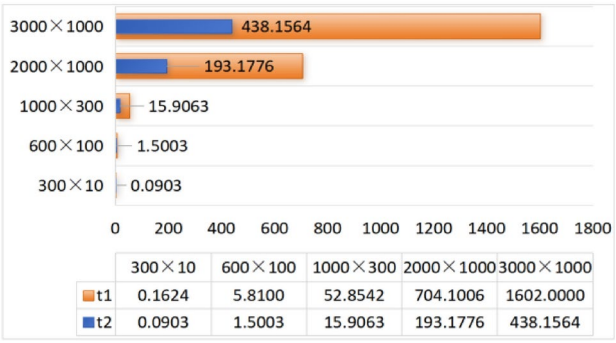

	300×10	600×100	1000×300	2000×1000	3000×1000
t1	0.1624	5.8100	52.8542	704.1006	1602.0000
t2	0.0903	1.5003	15.9063	193.1776	438.1564

Fig. 13. CPU time to calculate equivalent resistance using formula (1) and formula (6), respectively.

When $y_1 = 50$, $r/r_0 = 0.01$, the CPU time spent calculating the equivalent resistance by formula (1) and formula (6), respectively is shown in Fig. 14.

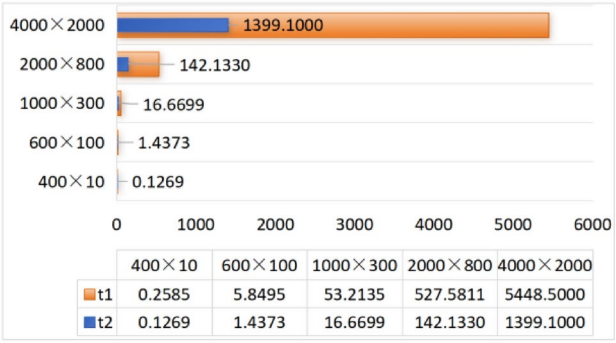

	400×10	600×100	1000×300	2000×800	4000×2000
t1	0.2585	5.8495	53.2135	527.5811	5448.5000
t2	0.1269	1.4373	16.6699	142.1330	1399.1000

Fig. 14. CPU time to calculate equivalent resistance using formula (1) and formula (6), respectively.

It can be clearly seen from the above six visualization charts that the computational efficiency of the improved formula (6) is higher than that of formula (1), and as the scale of the resistor network increases, the advantages of formula (6) become more obvious. As the resistivity decreases, the size of the data that can be processed using the equivalent resistance formula increases.

Conclusion

This paper uses Chebyshev polynomial of the second kind to improve the equivalent resistance formula of the $m \times n$ rectangular resistor network. Some special and interesting equcations of the resistor network, such as Eqs. (38), (44), (46), (47), (49) and (50) were introduced. To provide a visual representation, their three-dimensional views were plotted using MATLAB. Finally, several comparison tables were provided to show the calculation efficiency of two equivalent resistance formulas. The design philosophy and formulas presented in this study will inspire further research in fields such as neural networks and other related areas.

Data availibility

All data generated or analysed during this study are included in this article.

Received: 13 April 2024; Accepted: 22 November 2024
Published online: 27 November 2024

References

1. Tan, Z.-Z., Zhou, L. & Yang, J.-H. The equivalent resistance of a $3 \times n$ cobweb network and its conjecture of an $m \times n$ cobweb network. *J. Phys. A: Math. Theor.* **46**(19), 195202 (2013).
2. Tan, Z.-Z. Recursion-transform method to a non-regular $m \times n$ cobweb with an arbitrary longitude. *Sci. Rep.* **5**, 11266 (2015).
3. Tan, Z.-Z., Essam, J. W. & Wu, F. Y. Two-point resistance of a resistor network embedded on a globe. *Phys. Rev. E.* **90**(1), 012130 (2014).
4. Essam, J. W., Tan, Z.-Z. & Wu, F. Y. Resistance between two nodes in general position on an $m \times n$ fan network. *Phys. Rev. E.* **90**(3), 032130 (2014).
5. Tan, Z.-Z. & Fang, J.-H. Two-point resistance of a cobweb network with a $2r$ boundary. *Commun. Theor. Phys.* **63**(1), 36–44 (2015).
6. Tan, Z.-Z. Theory on resistance of $m \times n$ cobweb network and its application. *Int. J. Circ. Theor. Appl.* **43**(11), 1687–1702 (2015).
7. Tan, Z.-Z. Two-point resistance of an $m \times n$ resistor network with an arbitrary boundary and its application in RLC network. *Chin. Phys. B* **25**(5), 050504 (2016).

8. Tan, Z.-Z. Recursion-transform method and potential formulae of the $m \times n$ cobweb and fan networks. *Chin. Phys. B* **26**(9), 090503 (2017).
9. Tan, Z., Tan, Z.-Z. & Chen, J. Potential formula of the nonregular $m \times n$ fan network and its application. *Sci. Rep.* **8**, 5798 (2018).
10. Tan, Z. & Tan, Z.-Z. Potential formula of an $m \times n$ globe network and its application. *Sci. Rep.* **8**(1), 9937 (2018).
11. Hadad, Y., Soric, J. C. & Khanikaev, A. B. Self-induced topological protection in nonlinear circuit arrays. *Nat. Electron.* **1**, 178–182 (2018).
12. Zhang, D. et al. Impact damage localization and mode identification of CFRPs panels using an electric resistance change method. *Compos. Struct.* **276**, 114587 (2021).
13. Kirchhoff, G. Ueber die Aufölsung der Gleichungen, auf welche man bei der Untersuchung der linearen Vertheilung galvanischer Ströme geführt wird. *Ann. Phys.* **148**, 497–508 (1847).
14. Winstead, V. & Demarco, C. L. Network essentiality. *IEEE T. Circ.-I.* **60**(3), 703–709 (2012).
15. Ferri, G. & Antonini, G. Ladder-network-based model for interconnects and transmission lines time delay and cutoff frequency determination. *J. Circuit. Syst. Comp.* **16**, 489–505 (2007).
16. Owaidat, M. Q., Hijjawi, R. S. & Khalifeh, J. M. Network with two extra interstitial resistors. *Int. J. Theor. Phys.* **51**, 3152–3159 (2012).
17. Kirkpatrick, S. Percolation and conduction. *Rev. Mod. Phys.* **45**, 497–508 (1973).
18. Pennetta, C. et al. Biased resistor network model for electromigration failure and related phenomena in metallic lines. *Phys. Rev. B* **70**, 174305 (2004).
19. Kook, W. Combinatorial Green's function of a graph and applications to networks. *Adv. Appl. Math.* **46**, 417–423 (2011).
20. Shi, Y. et al. Novel discrete-time recurrent neural networks handling discrete-form time-variant multi-augmented Sylvester matrix problems and manipulator application. *IEEE Trans. Neur. Net. Lear.* **33**(2), 587–599 (2022).
21. Shi, Y., Zhao, W.-H., Li, S., Li, B. & Sun, X.-B. Novel discrete-time recurrent neural network for robot manipulator: a direct discretization technical route. *IEEE Trans. Neur. Net. Lear.* **34**(6), 2781–2790 (2021).
22. Liu, K.-P. et al. Five-step discrete-time noise-tolerant zeroing neural network model for time-varying matrix inversion with application to manipulator motion generation. *Eng. Appl. Artif. Intel.* **103**, 104306 (2021).
23. Sun, Z.-B. et al. Noise-suppressing zeroing neural network for online solving time-varying matrix square roots problems: A control-theoretic approach. *Expert. Syst. Appl.* **192**, 116272 (2022).
24. Jin, L., Qi, Y.-M., Luo, X., Li, S. & Shang, M.-S. Distributed competition of multi-robot coordination under variable and switching topologies. *IEEE Trans. Autom. Sci. Eng.* **19**(4), 3575–3586 (2022).
25. Jin, L., Zhang, Y.-N., Li, S. & Zhang, Y.-Y. Modified ZNN for time-varying quadratic programming with inherent tolerance to noises and its application to kinematic redundancy resolution of robot manipulators. *IEEE Trans. Ind. Electron.* **63**(11), 6978–6988 (2016).
26. Jin, L., Zheng, X. & Luo, X. Neural dynamics for distributed collaborative control of manipulators with time delays. *IEEE-CAA J. Autom.* **9**(5), 854–863 (2022).
27. Wang, X., Che, M. & Wei, Y. Complex-valued neural networks for the Takagi vector of complex symmetric matrices. *Neuron* **223**, 77–85 (2017).
28. Klein, D. J. & Randi, M. Resistance distance. *J. Math. Chem.* **12**, 81–95 (1993).
29. Giordano, S. Disordered lattice networks: general theory and simulations. *Int. J. Circ. Theor. Appl.* **33**, 519–540 (2005).
30. Wu, F. Y. Theory of resistor networks: the two-point resistance. *J. Phys. A: Math. Gen.* **37**, 6653 (2004).
31. Tzeng, W. J. & Wu, F. Y. Theory of impedance networks: the two-point impedance and LC resonances. *J. Phys. A: Math. Gen.* **39**, 8579 (2006).
32. Essam, J. W. & Wu, F. Y. The exact evaluation of the corner-to-corner resistance of an $M \times N$ resistor network: asymptotic expansion. *J. Phys. A: Math. Theor.* **42**, 025205 (2008).
33. Izmailian, N. S. & Huang, M.-C. Asymptotic expansion for the resistance between two maximum separated nodes on an M by N resistor network. *Phys. Rev. E.* **82**, 011125 (2010).
34. Lai, M.-C. & Wang, W.-C. Fast direct solvers for Poisson equation on 2D polar and spherical geometries. *Numer. Meth. Part. D. E.* **18**, 56–68 (2002).
35. Borges, L. & Daripa, P. A fast parallel algorithm for the Poisson equation on a disk. *J. Comput. Phys.* **169**, 151–192 (2001).
36. Izmailian, N. S., Kenna, R. & Wu, F. Y. The two-point resistance of a resistor network: a new formulation and application to the cobweb network. *J. Phys. A: Math. Theor.* **47**, 035003 (2014).
37. Izmailian, N. S. & Kenna, R. A generalised formulation of the Laplacian approach to resistor networks. *J. Stat. Mech: Theor. E.* **9**, 1742–5468 (2014).
38. Izmailian, N. S. & Kenna, R. The two-point resistance of fan networks. *Chin. J. Phys.* **53**(2), 040703 (2015).
39. Chair, N. Trigonometrical sums connected with the chiral Potts model, verlinde dimension formula, two-dimensional resistor network, and number theory. *Ann. Phys.* **341**, 56–76 (2014).
40. Chair, N. The effective resistance of the N-cycle graph with four nearest neighbors. *J. Stat. Phys.* **154**, 1177–1190 (2014).
41. Cserti, J. Application of the lattice Green's function for calculating the resistance of an infinite network of resistors. *Am. J. Phys.* **68**, 896–906 (2000).
42. Kook, W. Combinatorial Green's function of a graph and applications to networks. *Adv. Appl. Math.* **46**, 417–433 (2011).
43. Katsura, S. & Inawashiro, S. Lattice Green's functions for the rectangular and the square lattices at arbitrary points. *J. Math. Phys.* **12**, 1622 (1971).
44. Bairamkulov, R. & Friedman, E. G. Effective resistance of finite two-dimensional grids based on infinity mirror technique. *IEEE T. Circuits-I* **67**(9), 3224–3233 (2020).
45. Bairamkulov, R. & Friedman, E. G. Effective resistance of two-dimensional truncated infinite mesh structures. *IEEE T. Circuits-I* **66**(11), 4368–4376 (2019).
46. Kose, S. & Friedman, E. G. Effective resistance of a two layer mesh. *IEEE T. Circuits-II* **58**(11), 739–743 (2011).
47. Jiang, X.-Y., Zhang, G.-J., Zheng, Y.-P. & Jiang, Z.-L. Explicit potential function and fast algorithm for computing potentials in $\alpha \times \beta$ conic surface resistor network. *Expert. Syst. Appl.* **238**, 122157 (2024).
48. Zhou, Y.-F., Zheng, Y.-P., Jiang, X.-Y. & Jiang, Z.-L. Fast algorithm and new potential formula represented by Chebyshev polynomials for an $m \times n$ globe network. *Sci. Rep.* **12**(1), 21260 (2022).
49. Jiang, Z.-L., Zhou, Y.-F., Jiang, X.-Y. & Zheng, Y.-P. Analytical potential formulae and fast algorithm for a horn torus resistor network. *Phys. Phys. E.* **107**(4), 044123 (2023).
50. Zhou, Y.-F., Jiang, X.-Y., Zheng, Y.-P. & Jiang, Z.-L. Exact novel formulas and fast algorithm of potential for a hammock resistor network. *Aip. Adv.* **13**, 9 (2023).
51. Zhao, W.-J., Zheng, Y.-P., Jiang, X.-Y. & Jiang, Z.-L. Two optimized novel potential formulas and numerical algorithms for $m \times n$ cobweb and fan resistor networks. *Sci. Rep.* **13**(1), 12417 (2023).
52. Meng, X., Jiang, X.-Y., Zheng, Y.-P. & Jiang, Z.-L. A novel formula for representing the equivalent resistance of the $m \times n$ cylindrical resistor network. *Sci. Rep.* **14**(1), 21254 (2024).
53. Wang, J.-J., Zheng, Y.-P. & Jiang, Z.-L. Norm equalities and inequalities for tridiagonal perturbed toeplitz operator matrices. *J. Appl. Anal. Comput.* **13**(2), 671–683 (2023).
54. Fu, Y.-R., Jiang, X.-Y., Jiang, Z.-L. & Jhang, S. Inverses and eigenpairs of tridiagonal Toeplitz matrix with opposite-bordered rows. *J. Appl. Anal. Comput.* **10**(4), 1599–1613 (2020).

55. Fu, Y.-R., Jiang, X.-Y., Jiang, Z.-L. & Jhang, S. Analytic determinants and inverses of Toeplitz and Hankel tridiagonal matrices with perturbed columns. *Spec. Matrices.* **8**, 131–143 (2020).
56. Wei, Y.-L., Zheng, Y.-P., Jiang, Z.-L. & Shon, S. The inverses and eigenpairs of tridiagonal Toeplitz matrices with perturbed rows. *J. Appl. Math. Comput.* **68**, 623–636 (2022).
57. Wei, Y.-L., Jiang, X.-Y., Jiang, Z.-L. & Shon, S. On inverses and eigenpairs of periodic tridiagonal Toeplitz matrices with perturbed corners. *J. Appl. Anal. Comput.* **10**(1), 178–191 (2020).
58. Wei, Y.-L., Zheng, Y.-P., Jiang, Z.-L. & Shon, S. A study of determinants and inverses for periodic tridiagonal Toeplitz matrices with perturbed corners involving Mersenne numbers. *Mathematics.* **7**(10), 893 (2019).
59. Wei, Y.-L., Jiang, X.-Y., Jiang, Z.-L. & Shon, S. Determinants and inverses of perturbed periodic tridiagonal Toeplitz matrices. *Adv. Differ. Equ.* **2019**(1), 410 (2019).
60. Jiang, Z.-L., Wang, W.-P., Zheng, Y.-P., Zuo, B.-S. & Niu, B. Interesting explicit expressions of determinants and inverse matrices for Foeplitz and Loeplitz Matrices. *Mathematics.* **7**(10), 939 (2019).
61. Meng, Q.-Y., Zheng, Y.-P. & Jiang, Z.-L. Exact determinants and inverses of (2,3,3)-Loeplitz and (2,3,3)-Foeplitz matrices. *Comput. Appl. Math.* **41**, 35 (2022).
62. Meng, Q.-Y., Zheng, Y.-P. & Jiang, Z.-L. Determinants and inverses of weighted Loeplitz and weighted Foeplitz matrices and their applications in data encryption. *J. Appl. Math. Comput.* **68**, 3999–4015 (2022).
63. Meng, Q.-Y., Jiang, X.-Y. & Jiang, Z.-L. Interesting determinants and inverses of skew Loeplitz and Foeplitz matrices. *J. Appl. Anal. Comput.* **11**, 2947–2958 (2021).
64. Horadam, A. F. Basic properties of a certain generalized sequence of numbers. *Fibonacci Q.* **3**, 161–176 (1965).
65. Udrea, G. A note on the sequence $(W_n)_{n\geq 0}$ of A.F. *Horadam. Port. Math.* **53**, 143–156 (1996).
66. Mason, J. C., Handscomb, D. C. *Chebyshev Polynomials* (Chapman & Hall, 2002).
67. Garcia, S. R. & Yih, S. Supercharacters and the discrete Fourier, cosine, and sine transforms. *Commun. Algebra.* **46**(9), 3745–3765 (2018).
68. Sanchez, V., Peinado, A. M., Segura, J. C., Garcia, P. & Rubio, A. J. Generating matrices for the discrete sine transforms. *IEEE T. Signal. Process.* **44**(10), 2644–2646 (1996).

Acknowledgements

The research was Supported by the National Natural Science Foundation of China (Grant No.12101284), the Natural Science Foundation of Shandong Province (Grant No. ZR2022MA092) and the Department of Education of Shandong Province (Grant No.2023KJ214).

Author contributions

Xiao-Yu, Jiang and Yan-Peng, Zheng conceived the project, performed and analyzed formulae calculations. Ru, Wang and De-liang, Xiang validated the correctness of the formula calculation, and realized graph drawing. Zhao-Lin, Jiang proposed an improved formula for calculating equivalent resistance. All authors contributed equally to the manuscript.

Competing interests

The authors declare no competing interests.

Additional information

Correspondence and requests for materials should be addressed to X.J. or Y.Z.